Pressure-Induced Unfolding/Refolding of Ribonuclease A: Static and Kinetic Fourier Transform Infrared Spectroscopy Study†

Gunda Panick and Roland Winter*

Department of Chemistry, Physical Chemistry I, University of Dortmund, Otto-Hahn-Strasse 6, D-44227 Dortmund, Germany

Received September 20, 1999; Revised Manuscript Received November 15, 1999

ABSTRACT: In this paper, we illustrate the use of high-pressure Fourier transform infrared (FT-IR) spectroscopy to study the reversible presssure-induced unfolding and refolding of ribonuclease A (RNase A) and compare it with the results obtained for the temperature-induced transition. FT-IR spectroscopy monitors changes in the secondary structural properties (amide I′ band) or tertiary contacts (tyrosine band) of the protein upon pressurization or depressurization. Analysis of the amide I′ spectral components reveals that the pressure-induced denaturation process sets in at 5.5 kbar at 20 °C and pH 2.5. It is accompanied by an increase in disordered structures while the content of β-sheets and α-helices drastically decreases. The denatured state above 7 kbar retains nonetheless some degree of β-like secondary structure and the molecule cannot be described as an extended random coil. Increase of pH from 2.5 to 5.5 has no influence on the structure of the pressure-denatured state; it slightly changes the stability of the protein only. All experimental evidence indicates that the pressure-denatured states of monomeric proteins have more secondary structure than the temperature-denatured states. Different modes of denaturation, including pressure, may correlate differently with the roughness of the energy scale and slope of the folding funnel. For these reasons we have also carried out pressure-jump kinetic studies of the secondary structural evolution in the unfolding/refolding reaction of RNase A. In agreement with the theoretical model presented by Hummer et al. [(1998) *Proc. Natl. Acad. Sci. U.S.A. 95*, 1552−1555], the experimental data show that pressure slows down folding and unfolding kinetics (here 1−2 orders of magnitude), corresponding to an increasingly rough landscape. The kinetics remains non-two-state under pressure. Assuming a two-step folding scenario, the calculated relaxation times for unfolding of RNase A at 20 °C and pH 2.5 can be estimated to be $\tau_1 \approx 0.7$ min and $\tau_2 \approx 17$ min. The refolding process is considerably faster ($\tau_1 \approx 0.3$ min, $\tau_2 \approx 4$ min). Our data show that the pressure stability and pressure-induced unfolding/refolding kinetics of monomeric proteins, such as wild-type staphylococcal nuclease (WT SNase) and RNase A, may be significantly different. The differences are largely due to the four disulfide bonds in RNase A, which stabilize adjacent structures. They probably lead to the much higher denaturation pressure compared to SNase, and this might also explain why the volume change of WT SNase upon unfolding is about twice as large.

Since Anfinsen et al. (*1*) first studied the renaturation of reduced and unfolded ribonuclease A (RNase A), much effort has been devoted to attempting to understand the relationship between the amino acid sequence, the structure, and unfolding/refolding reactions of proteins. Recently, increasing attention has been focused on denatured and partially folded states, since determination of their structure and stability may provide critical insights into the mechanisms of protein folding (*2*−*6*). A fundamental understanding of the process of the folding of proteins to their native state has fascinated protein chemists for many years and remains one of the most challenging issues in modern biophysics. Based on a huge body of experimental data, a number of models have been proposed for this process, such as diffusion-collision models (*6*, *7*), the hydrophobic collapse model (*8*), or the funnel model (*9*, *10*). For an in-depth discussion of various folding models and pathways the reader may consult, among others, refs *2*, *5*, and *11*−*15*.

Most studies dealing with protein denaturation have been carried out at atmospheric pressure with various physicochemical perturbations, such as temperature, pH, or chemical denaturants, as experimental variables. Besides temperature and chemical potential, pressure represents a further important thermodynamic variable and the volume changes obtained, which are associated with the observed transitions, correspond to a fundamental physical parameter of the protein−solvent system. Compared to varying temperature, which produces simultaneous changes in both density (or volume) and thermal energy, the use of pressure to study protein solutions perturbs the environment of the protein in a continuous, controlled way by changing intermolecular distances. As such, pressure represents a potentially very informative approach to the study of protein structure and

† Financial support by the Deutsche Forschungsgemeinschaft (DFG) is gratefully acknowledged.

* To whom correspondence should be addressed: Phone +49 231 755 3900; Fax: +49 231 755 3901; E-mail winter@steak.chemie.uni-dortmund.de.

10.1021/bi992176n CCC: $19.00
Published on Web 01/25/2000

stability. A more complete description of the pressure-denatured states of proteins, therefore, should be quite useful to the understanding of protein folding phenomena.

It has long been known that the application of hydrostatic pressure results in the disruption of native protein structure (*16*, *17*) due to the decrease in the total volume of the protein−solvent system upon unfolding. Pressure denaturation studies thus provide a fundamental thermodynamic parameter for protein unfolding, the volume change $\Delta V_u°$, in addition to an alternative method for perturbing the folded state, and thus extracting its stability, the free enthalpy change $\Delta G_u°$. A number of reviews on effects of pressure on proteins discuss these volume changes in greater detail (*18*−*22*). In a recent theoretical study the pressure dependence of the hydrophobic interactions has been shown to be consistent with the observed pressure denaturation of proteins (*23*).

In addition to being an important thermodynamic variable, pressure can also be used as a very valuable means of triggering and investigating the kinetics of the unfolding/refolding transition of proteins. The use of pressure as a kinetic variable for studying the kinetics of biomolecular phase transformations is a field that is developing rapidly (*22*, *24*). Generally, the pressure-jump technique has several advantages over other trigger mechanisms: (1) it does not significantly change the solvent properties, (2) pressure propagates rapidly so that sample homogeneity is no problem, and (3) pressure jumps can be performed bidirectionally, i.e., in both the pressurization and depressurization directions.

The structural properties of the denatured state achieved may depend on the method employed to perturb the native structure. Moreover, our grasp of these possible differences depends on the observable parameters used, and quantitative comparison of results between different techniques often is difficult. Recognizing that the denatured state achieved by any perturbation method likely corresponds to a relatively large ensemble of conformations, one can imagine that the free energy landscape of this denatured ensemble may be dependent upon pressure, temperature and chemical potential (i.e., denaturant activity).

There is yet another reason for systematic studies on the pressure unfolding of proteins related to the new theoretical approach by Bryngelson and Wolynes (*13*), which uses statistical characterization of the energy landscape in analyzing protein folding. Different modes of denaturation, including pressure, may correlate differently with the roughness of the energy scale and slope of the folding funnel. Small changes in the solvent temperature or pressure might lead to continuous changes in the populations of molecular conformations during folding. Such subtlety is not recognized in the classical modeling where specific intermediate structures and pathways are invoked.

In this paper, we first illustrate the use of high-pressure IR spectroscopy to study the reversible presssure-induced unfolding and refolding of RNase A and compare it with the results obtained for the temperature-induced transition. This work is a continuation of our studies on pressure-induced unfolding/refolding reactions of proteins (*25*, *26*). Our recent pressure-jump relaxation fluorescence, Fourier transform infrared (FT-IR), and small-angle X-ray scattering (SAXS) studies on staphylococcal nuclease (SNase) have brought to light that the effect of pressure on the kinetics arises from a larger positive activation volume for folding than for unfolding and leads to a significant slowing down of the folding rate with increasing pressure (*25*, *26*). In this case, the system becomes two-state under pressure. The large positive activation volume for folding was interpreted as an indication that the rate-limiting step in the folding of SNase involves dehydration of a significant proportion of the polypeptide chain. These studies provided a picture of the transition state in which a significant fraction of the protein has been removed from contact with the solvent.

To characterize the nature of the transition state in the pressure-induced folding/unfolding reaction of RNase A, a representative of a different class of monomeric proteins, we also performed pressure-jump kinetic FT-IR studies on this protein. RNase A is a single-domain protein, a pancreatic enzyme that catalyzes the cleavage of single-stranded RNA. This protein consists of 124 amino acid residues with a molecular mass of 13.7 kDa. The crystalline state of the protein contains about 23% helices, 46% β-sheets, 21% turns, and 10% unordered structures (*27*). The protein has traditionally served as a model for protein folding because it is small and stable and has a well-known native structure. The folding pathway of the protein has been studied extensively in the past. Several studies of RNase strongly suggest that its folding proceeds though intermediates, including an early hydrogen-bonded intermediate and a late nativelike intermediate (*28*−*35*). Experimental evidence suggests that nonrandom structures still exist in the denatured state. Among other studies, circular dichroism (CD) and FT-IR studies indicate that there is a significant amount of structure left in thermally denatured RNase A (*36*−*42*). A stable hydrogen-bonded structure could not be detected by amide proton protection experiments up to 65 °C (*43*).

MATERIALS AND METHODS

Bovine pancreatic ribonuclease A (RNase A) was purchased from Sigma Chemical Co. and used without further purification. The protein was dissolved in D_2O at pH 3, and the solution was heated to 55 °C for 20 min to allow for deuterium exchange of the labile amide protons of RNase A. The sample was then lyophilized from D_2O. This procedure was performed twice for each sample. The uncorrected pH values of D_2O solutions were adjusted with DCl (Sigma) and NaOD (MSD Isotopes). The RNase A was dissolved to a concentration of 4 mM in 20 mM maleic acid buffer and 0.3 M NaCl in 99.9% D_2O.

FT-IR spectroscopy has proven to be a very powerful technique to determine the secondary structure elements even under high-pressure conditions (*22*, *25*, *26*, *44*, *45*). The amide I band (between 1600 and 1700 cm^{-1}) has been studied, which is mainly associated with the C═O stretching vibration (70−85%) of the amide groups and which is directly related to the backbone conformation and hydrogen-bonding pattern. The FT-IR spectra were recorded with a Nicolet Magna 550 spectrometer equipped with a liquid nitrogen-cooled HgCdTe-detector. For the pressure-dependent measurements the infrared light was focused by a spectra bench onto the pinhole of the diamond anvil cell (DAC) with type IIa diamonds (*46*). Each spectrum was obtained by coadding 512 scans at a spectral resolution of 2 cm^{-1} and was apodized with a Happ−Genzel function. The sample chamber was purged with dry and carbon dioxide-free air.

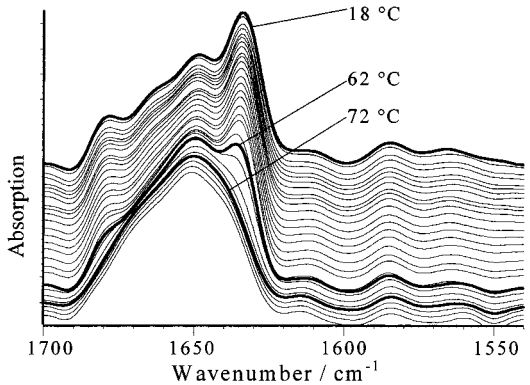

FIGURE 1: Deconvoluted FT-IR absorption spectra of RNase [5% (w/w), pH 2.5] as a function of temperature at ambient pressure.

Powdered α-quartz was placed in the hole of the steel gasket and changes in pressure were quantified by the shift of the quartz phonon band at 695 cm^{-1} (*47*). Precise pressure studies of a sample in a diamond anvil cell can be performed only unidirectionally, in the pressurization direction, so we present no data in the depressurization direction. The thermal denaturation of RNase was measured in a cell with CaF_2 windows separated by 25 μm Teflon spacers. An external water thermostat was used for pressure- and temperature-dependent measurements to control the temperature within 0.1 °C. The equilibration times to take one data point at each temperature and pressure was about 15 min. Pressure jumps were obtained by turning the spring-loaded screw of the DAC.

Fourier self-deconvolution of the IR spectra was performed with a resolution enhancement factor of 1.8 and a bandwidth of 15 cm^{-1}. The fractional intensities of the secondary structure elements were calculated from a band-fitting procedure assuming a Gaussian−Lorentzian line shape function (*48*, *49*).

To determine the standard Gibbs free energy change $\Delta G_u°$ and the volume change $\Delta V_u° = d\Delta G_u°/dp$ of a two-state pressure-induced unfolding process, the equilibrium profiles obtained from the FT-IR spectra can be fitted to $\Delta G_u° = -RT \ln K_{eq,u} = -RT \ln[(I_f - I_p)/(I_p - I_u)]$ using the data points at each pressure, I_p, and the asymptotic values of the fractional band intensities due to particular secondary structural elements for the folded and unfolded states, I_f and I_u, respectively.

RESULTS

Temperature Dependence of the Amide I′ FT-IR Spectrum of RNase A. For comparison with the pressure-induced unfolding data, we show in Figure 1 deconvoluted IR spectra of RNase A between 18 and 82 °C at pH 2.5 and ambient pressure after H/D exchange at 55 °C. At 20 °C, the maximum of the amide I′ band (the prime indicates that the solvent is D_2O) occurs at 1637 cm^{-1}. Increase of temperature to 82 °C leads to a shift of the band maximum to larger wavenumbers and the absorption band becomes more symmetric.

Also the IR absorption band position of the tyrosine aromatic ring (at 1514 cm^{-1}) increases (data not shown). Generally, tyrosine absorbance monitors formation of tertiary structure contacts during folding, whereas the amide I′ band monitors formation of secondary structures, although it may also be sensitive to later formation of tertiary structure. Tyrosine absorbance changes are thus observed when hydrophobic cores of the protein are formed, as solvent is excluded from the vicinity of tyrosine residues that are buried in native protein. Three of the six tyrosines in RNase A (Y25, Y73, and Y97) are known to be buried in the native molecule whereas the other three (Y76, Y 92, and Y115) are located on the protein surface.

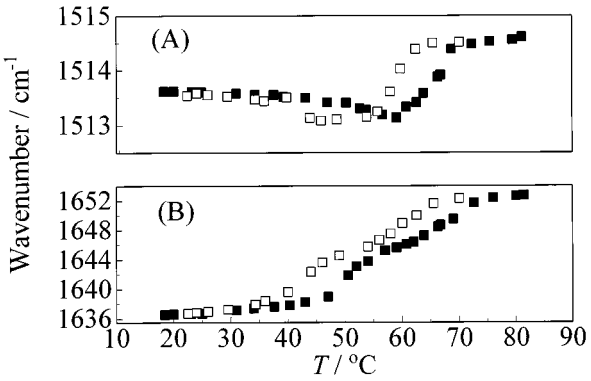

FIGURE 2: Temperature effect on the maximum of the tyrosine (A) and amide I′ (B) IR absorption band (■, heating direction; □, cooling direction).

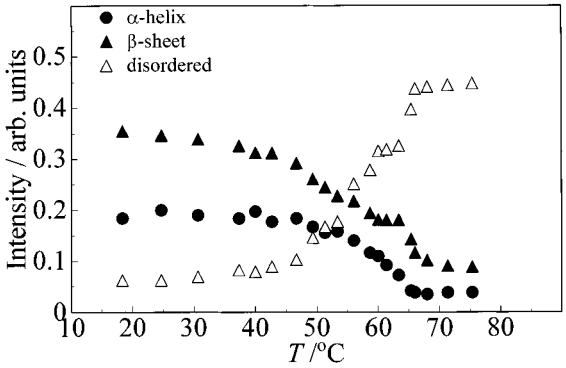

FIGURE 3: Temperature effect on the areas of the bands associated with β-sheets, α-helices, and disordered structures of RNase A at pH 2.5 and ambient pressure.

To determine the location of the temperature-induced unfolding of the protein, the position of the amide I′ and tyrosine bands are shown as a function of temperature in Figure 2. Increase of temperature to 45 °C leads to a small increase of the amide I′ band frequency. Above that temperature it increases in two steps, around 47 and 64 °C, respectively.

The tyrosine band position first slightly decreases with increasing temperature up to 47 °C, and from there on more drastically up to 60 °C, from where it increases up to a plateau value that is reached at about 72 °C. This behavior indicates that at about 60 °C only part of the tertiary structure has unfolded and complete unfolding is reached above 70 °C. The process is completely reversible up to temperatures of 76 °C; a hysteresis of a few degrees only is observed.

The evolution of the secondary structures with temperature is shown in Figure 3. The secondary structure elements are assigned to IR bands as summarized in Table 1. The temperature-induced decrease of band intensities of β-sheets and α-helices between 50 and 70 °C is accompanied by an increase in band intensities of nonperiodic and turn structures. The nonmonotonic changes in the component intensities as

Table 1: Assignment of Observed RNase A Infrared Bands[a]

band position (cm^{-1})	assignment
1633	β-sheets
1645	disordered
1652	α-helices
1663	turns
1672	turns
1680	β-sheets

[a] Infrared bands were observed at 25 °C in D_2O Buffer Solution after H/D Exchange (*41*, *64*).

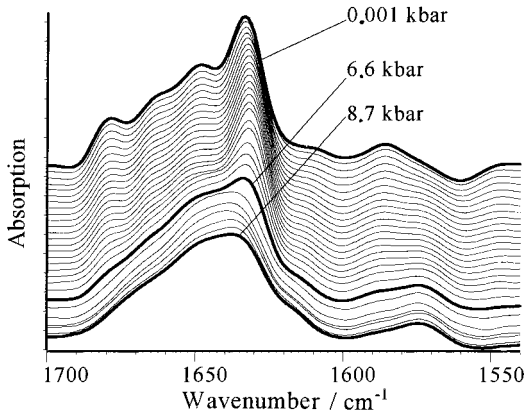

FIGURE 4: Deconvoluted FT-IR absorption spectra of RNase A [5% (w/w), pH 2.5] at 20 °C as a function of pressure.

a function of temperature point to more steps in the unfolding process. Also, in Raman spectroscopic investigations a multistep behavior has been observed (*50*). Our IR data indicate that the level of ordered secondary structure elements at temperatures above 70 °C is very low or almost negligible (at least a 75% decrease).

We also performed measurements at pH 5.5 between 20 and 90 °C (data not shown). The tyrosine band is shifted about 1 cm^{-1} to higher frequencies at pH 5.5, the amide I′ band position is unchanged, however. At pH 5.5 the first step in the unfolding process in the amide I′ data sets in at a slighly higher temperature (ca. 55 °C at pH 5.5, compared to ca. 47 °C at pH 2.5); otherwise no changes are observed. Within the accuracy of the experiment, also the intensities of the secondary structure elements in the native and unfolded state are similar at pH 2.5 and 5.5, respectively.

Pressure Dependence of the Amide I′ FT-IR Spectrum of RNase A. To investigate the effect of pressure on the secondary structure of RNase A, we measured the pressure-induced changes in the amide I′ region of the infrared spectrum in the pressure range from 1 bar to 10 kbar. The deconvoluted FT-IR spectra of deuterium exchanged RNase A at pH 2.5 and 20 °C are shown in Figure 4. The data reveal a reversible conformational transition of RNase A in the pressure range around 6−7 kbar at this temperature. The asymmetric amide I′ band becomes more symmetric with a band maximum at 1643 cm^{-1}. The pressure dependence of the band maxima of the amide I′ and tyrosine bands is depicted in Figure 5. Both band positions change significantly in the pressure range between 5.5 and 6.5 kbar and at a similar position. The pressure-induced changes in the secondary structures thus seem to coincide largely with that of the local structure around the tyrosine groups.

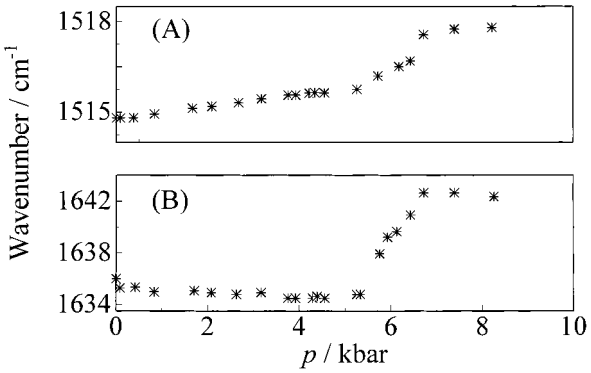

FIGURE 5: Pressure effect on the maximum of the tyrosine (A) and amide I′ (B) IR absorption band of RNase A [5% (w/w), pH 2.5] at $T = 20$ °C.

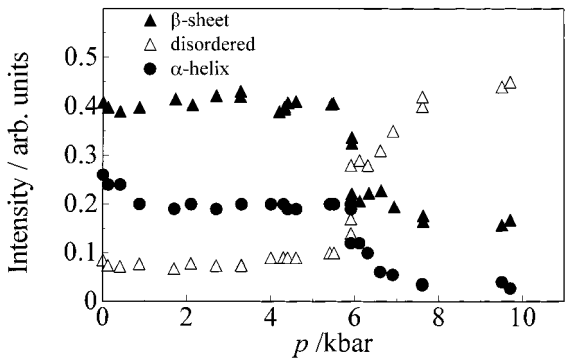

FIGURE 6: Pressure effect on the areas of the bands associated with β-sheets, α-helices, and disordered structures of RNase A at pH 2.5 and 20 °C.

The changes of the fractional intensities of the different amide I′ subbands are presented in Figure 6. The pressure-induced denaturation as judged by changes in the fractional band intensities begins at 4.5 kbar and the transition is complete at about 7.5 kbar. Although the fractional intensities of α-helices and β-sheets decrease significantly, these structures, in particular the β-sheet structures, are not completely disrupted by pressure. A similar behavior is observed at pH 5.5. At the higher pH value, the transition is shifted to slightly higher pressures (ca. 0.5 kbar) only. At pH 5.5 the tyrosine band position is shifted by 1 cm^{-1} to higher wavenumbers compared to that at pH 2.5. Increase of pH from 2.5 to 5.5 thus has no influence on the structure of the pressure-denatured state; it slightly changes the stability of RNase A only.

Assuming the pressure-induced unfolding transition of RNase A could be treated as a simple two-state process, we obtain a Gibbs free energy change for unfolding of $\Delta G_u^\circ = 27 \pm 5$ kJ/mol and a volume change for unfolding of $\Delta V_u^\circ = -45 \pm 8$ mL/mol at ambient temperature and pressure. A similar volume change has been observed at pH 2 (*51*). With increasing temperature, ΔV_u° has been found to become less negative (*52*). For comparison, the corresponding data obtained for unfolding of SNase WT are 16 ± 4 kJ/mol and -80 ± 20 mL/mol (*25*, *26*). The volume change of SNase WT upon unfolding is thus about twice that of RNase A.

*Time Dependence of the Amide I′ FT-IR Spectrum of RNase A after a Pressure Jum*p. To study the unfolding and refolding kinetics of RNase A, pressure jumps from 5 to 7.5 kbar and from 7.5 to 0.001 kbar have been performed. Figure 7 shows the corresponding deconvoluted infrared spectra at

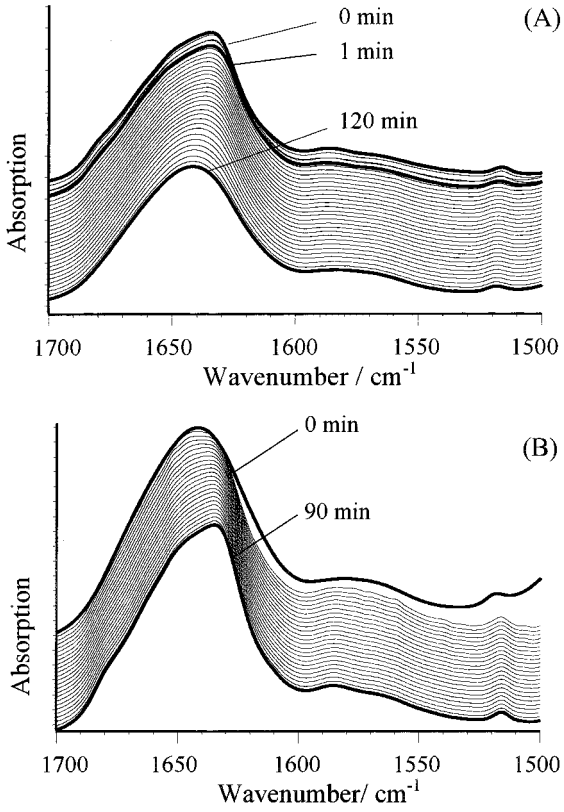

FIGURE 7: Deconvoluted FT-IR absorption spectra of RNase A as a function of time after a *p*-jump from 5 to 7.5 kbar (A) and from 7.5 kbar to 1 bar (B) (T = 20 °C, pH 2.5).

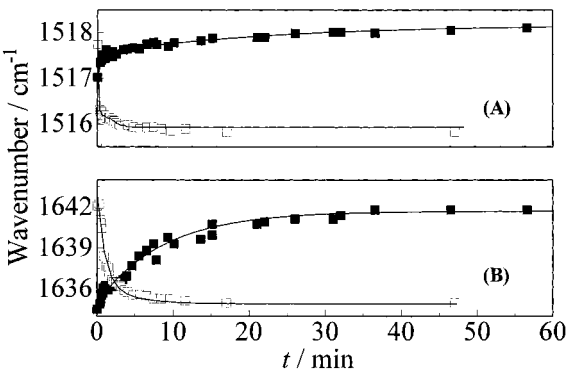

FIGURE 8: Time dependence of the position of the tyrosine band (A) and the maximum of the amide I′ band (B) of RNase A after a *p*-jump from 5 to 7.5 kbar (■), and from 7.5 to 0.001 kbar (□) (T = 20 °C, pH 2.5).

T = 20 °C. The data reveal a significant change in the shape of the IR spectra on the time scale of minutes after the pressure jump. The amide I′ band becomes more symmetrical after the pressure jump into the denatured state and the tyrosine band is shifted toward higher wavenumbers. Release of pressure from 7.5 kbar to 1 bar leads to a recovering of the FT-IR band shape (Figure 7 B). The first IR spectrum after the *p*-jump is already different from the one before the jump, indicating a fast burst phase that cannot be resolved here. The dead time of the current high-pressure kinetic FT-IR experiment is about 20 s.

Figure 8 shows the maximum of the tyrosine and amide I′ band position as a function of time after *p*-jumps from 5 to 7.5 kbar and from 7.5 kbar to 1 bar at T = 20 °C. After the *p*-jump from 5 to 7.5 kbar, the position of the amide I′

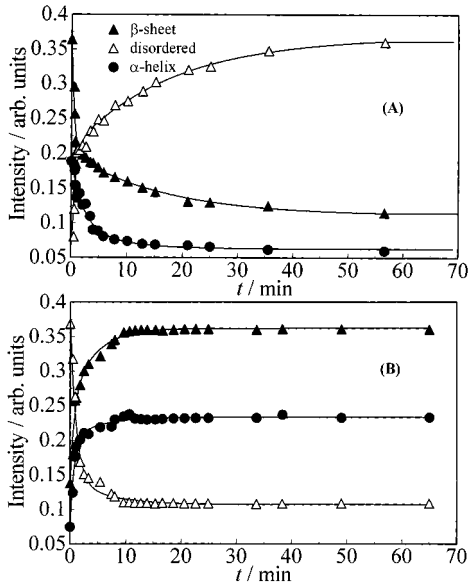

FIGURE 9: Time-dependent fractional intensities of secondary structure elements of RNase A after a *p*-jump from 5 to 7.5 kbar (A) and from 7.5 kbar to 1 bar (B) at T = 20 °C and pH 2.5.

band shifts 6 cm^{-1} to larger wavenumbers within 20−30 min. Interestingly, the time dependence of the tyrosine band is different—it develops much faster. Such behavior is probably due to a prior change in the direct vicinity of some of the six tyrosine residues, likely the burried ones. In the case of WT SNase (*26*), both bands change on a similar time scale. This indicates that the time evolution for the secondary structures in RNase A is different from the local changes around the tyrosine groups. Similar behavior is observed when the pressure is released and the refolding of the protein is observed.

CONCLUSIONS

The FT-IR measurements indicate that the thermally denatured state of RNase A still retains some secondary structure and is reversible up to temperatures as high as 76 °C. The data further indicate that at about 60 °C only part of the tertiary structure has unfolded and complete unfolding is reached above 70 °C. Also, previous thermal equilibrium studies of the unfolding and folding of RNase A have provided evidence for the presence of intermediates in denaturation at low pH (*36*−*42*, *50*, *53*). SAXS and FT-IR data of Sosnick and Trewhella (*42*) indicate that the temperature-denatured state at 67 °C still has a compact structure with some residual secondary structure. They also demonstrate that the thermal denaturation in RNase A is not a simple two-state transition from a native to a completely disordered random coil structure. The radius of gyration R_g increases from 15 Å at room temperature to about 19 Å at 67−81 °C for RNase A at pD = 5.7. A random coil conformation could be expected to have an R_g value greater than 41 Å (*54*). The existence and maintenance of a compact shape by the protein, which is different from, e.g., SNase (*25*, *26*), might be attributed to the presence of the four disulfide bonds between the eight cysteine residues. Up to 65 °C, significant amounts of secondary structure have been observed by Seshadri et al. (*41*), which is in accordance with our data. IR data by Fabian and Mantch (*55*) indicate that the thermal unfolding of RNase A is reversible over the pH

range 2.1−7.4; even at high protein concentrations of 2 mg/40 mL of solvent, the heat-denatured RNase A does not contain any significant amount of authentic hydrogen-bonded secondary structures, however.

Reversible pressure unfolding/refolding experiments have been carried out at pH 2.5 and 5.5 and 20 °C in the pressure range from 1 bar to 10 kbar. The results indicate that the protein unfolds at a rather high pressure (about 6 kbar at pH 2.5), and the pressure-denatured state contains partially folded structures (ca. 30 %). This seems to be a general finding. So far, all experimental evidence indicates that the pressure-denatured states of proteins have more secondary structure than the temperature-denatured states. Contrary to the temperature-dependent data, the pressure data of RNase A indicate that the pressure-induced equilibrium changes in the secondary structures seem to coincide essentially with those of the local structure around the tyrosine groups.

Reversible pressure denaturation experiments on RNase A by NMR techniques have been carried out by Jonas and co-workers (*56*) at pH 2.0 and 10 °C in the pressure range from 1 bar to 5 kbar. In these studies the histidine resonances have been followed. It was found that His 12 unfolds first but retains a partially folded environment, even in the completely pressure-denatured state. Then the regions near His 48 and His 105 unravel, behavior that is similar to the thermal denaturation and the denaturation induced by urea or guanidine hydrochloride. They also found that the structure of the pressure-denatured protein at low pH is far from completely unfolded. They further concluded that hydrogen exchange is slower in the center of the β-sheet of the native protein than at the end and that some of the residues with large protection factors are those near the disulfide bonds. It has been pointed out recently that these residual structures may resemble folding intermediates or serve as initial sites for protein folding (*57*, *58*). So one might assume that the structure of the pressure-denatured RNase A resembles that of the early intermediate found in temperature-jump experiments (*35*).

Compared to WT SNase, which unfolds at about 2 kbar at 20 °C, the denaturation pressure of RNase A is very high. It is likely that the covalent disulfide bonds in RNase A cannot be broken easily by these pressures, and the disulfide bonds stabilize adjacent structures and protect them against further unfolding. They might also lead to the much higher denaturation pressure compared to that of SNase. This might also explain why the volume change of SNase WT upon unfolding is about twice as large.

These findings are also in accordance with recent high-pressure SAXS data by Kleppinger et al. (*59*), which show that there is only a small change occurring in the radius of gyration of RNase A (at pH 7.8, 100 mg/mL), from 17 Å at ambient pressure to about 27 Å in the pressure-induced unfolded state at 8 kbar.

Several types of protein denaturation, especially thermal and chemical denaturation, leave little or no residual structure in many proteins. By contrast, pressure denaturation, which is a relatively mild way of denaturation, suggests that this method can leave appreciable residual structure in proteins. A similar conclusion has also been drawn from studies of other proteins. For example, Cléry et al. (*65*) studied the pressure denaturation of butyrylcholinesterase. They observed that the pressure denaturation is a multistep process and the observed transient pressure-denatured states have characteristics of molten globules. Peng et al. (*66*) also found that the conformation of the pressured-dissociated monomers of Arc repressor are typical of a molten globule and they showed that their structure is considerably different from that of the native dimer and the thermally denatured monomers. Similar behavior has also been observed for the residual structure in the pressure-assisted cold-denatured state of lysozyme by Nash et al. (*67*). If the activation barriers are not too high, these mildly denatured structures could be expected to be among the first to appear in the refolding process of the protein under ambient conditions. It is also likely that the equilibrium molten globules of some proteins, obtained under these mildly denaturing conditions, are structurally similar to the early collapsed states occurring when the protein begins to fold.

To study the pressure-induced unfolding/refolding kinetics, pressure jump relaxation experiments have been performed across the phase transition region of the protein. The IR data reveal significant changes in the shape of the IR spectra still on the time scale of minutes after the pressure jump. Differences in the time constants derived from the amide I′ band and from the tyrosine vibration were observed, indicating that the time evolution for the secondary structures is different from the local changes around the tyrosine groups. Within the accuracy of the experiment, these data fit well to a model assuming two exponential relaxation processes. The calculated relaxation times for unfolding of RNase A at 20 °C and pH 2.5 are $\tau_1 = 0.7 \pm 0.5$ min and $\tau_2 = 17 \pm 1.5$ min. The refolding process is considerably faster. The corresponding relaxation times are $\tau_1 = 0.3 \pm 0.3$ min and $\tau_2 = 4 \pm 0.8$ min, respectively.

For comparison, the urea and in particular the temperature-induced unfolding/refolding processes are much faster. Recently, significant progress has been made in the experimental realization of fast IR spectroscopic measurements for studying the unfolding/refolding transition of proteins. Thermally induced unfolding of RNase A was studied by applying laser-induced temperature jumps on the nanosecond time scale (*60*). In another approach, a fast injection attachment was developed to follow refolding of the protein after thermal denaturation in the millisecond to minute time scale with FT-IR spectroscopy (*61*). Also, a stopped-flow apparatus was developed for IR spectroscopy, permitting the investigation of unfolding and refolding processes of proteins initiated by chemical denaturants (*62*, *63*). Kinetic IR experiments applying a temperature jump or by rapid dilution of a urea solution containing the chemically unfolded protein were recently performed on the time scale of hundreds of milliseconds to minutes (*63*). These kinetic studies provide evidence for a high structural similarity of urea-denatured and heat-denatured RNase A. The kinetic infrared data demonstrate that in the time window of 0.1−30 s approximately 40% of the native β-sheet structure in RNase A is formed in the presence of 0.6 M urea at pH 3.6. Temperature-jump experiments in the absence of chemical denaturants exhibited faster (at least 2-fold) and more complex refolding kinetics. The temperature-induced refolding process of RNase A could also be described by a two-stage process, with relaxation times of 1.3 and 6.7 s, whereby the faster phase dominates over the slower phase. A kinetic folding intermediate of RNase A was also found in the early

stage (here within the first 1.5 s) of refolding by pulsed hydrogen-exchange NMR experiments (*31*, *32*). All NH protons that are hydrogen-bonded within the β-sheet of native RNase A seem to be protected in the intermediate.

In comparison, the pressure-induced relaxation times of unfolding and refolding of RNase A are much slower. This might be due to the large activation volumes of the unfolding and refolding process, allowing us to observe these processes without resorting to ultrafast methods. A similar behavior has been observed in our studies of WT SNase (*35*, *36*). However, our data show that the stability and unfolding/refolding kinetics of the two proteins are significantly different. The pressure-jump SAXS and FT-IR data, along with previous fluorescence pressure-jump results, provide strong evidence for a two-state folding/unfolding model for SNase under pressure (*25*, *26*), in that secondary structure, chain collapse, and tertiary structure all exhibit relaxation profiles on similar time scales. Thus, changes in these three order parameters appear to depend on the same rate-limiting steps for unfolding and refolding. In landscape terms, this means there are no basins where molecules collect, and there are no significant uphill slopes (increase in internal free energy) along the microscopic folding paths on the energy landscape. The results for this small, fast-folding protein thus conform relatively well to the type I scenario of the funnel model, with a relatively smooth funnel topology. In RNase A, a different scenario is observed. In this case the funnel topology does not seem to be as smooth. Not only the temperature-induced but also the pressure-induced unfolding/refolding reaction is a multistep process, at least two steps, pointing to a more rugged folding funnel.

Bryngelson et al. (*13*) already pointed out that pressure can be used to explore the roughness of the folding landscape, as by changing the experimental variable, the scenario of folding can be tuned. In agreement with the theoretical model presented by Hummer et al. (*23*), the experimental data obtained so far show that pressure slows down folding and unfolding kinetics, corresponding to an increasingly rough landscape and/or decrease in landscape stretching.

The fastest folding speed probably depends on the viscosity of the solvent, which could be tuned by pressure continuously. By use of a fast-folding simple protein exhibiting a smooth folding landscape, the effect of viscosity on the folding kinetics could be studied in future experiments. This should lead to a better theoretical understanding of the rate-limiting slope of the energy landscape.

REFERENCES

1. Anfinsen, C. B. (1973) *Science 181*, 223−230.
2. Kim, P. S., and Baldwin, R. L. (1990) *Annu. Rev. Biochem. 59*, 631−660.
3. Creighton, T. E. (1993) *Proteins*, W. H. Freeman & Co., New York.
4. Matthias, B., Radford, S. E., and Dobson, C. M. (1994) *J. Mol. Biol. 237*, 247−254.
5. Dobsen, C. M., Sali, A., and Karplus, M. (1998) *Angew. Chem. 110*, 908−935.
6. Kim, P. S., and Baldwin, R. L. (1982) *Annu. Rev. Biochem. 51*, 459−489.
7. Karplus, M., and Weaver, D. L. (1976) *Nature 260*, 404−406.
8. Dill, K. A., and Stigter, D. (1995) *Adv. Protein Chem. 46*, 59−104.
9. Onuchic, J. N., Wolynes, P. G., and Soccir, N. D. (1995) *Proc. Natl. Acad. Sci. U.S.A. 92*, 3626−3630.
10. Onuchic, J. N., Luthey-Schulten, Z., and Wolynes, P. G. (1997) *Annu. Rev. Phys. Chem. 48*, 545−600.
11. Richards F. M., and Lim W. A. (1994) *Annu. Rev. Biophys. Bioeng. 26*, 423−498.
12. Karplus, M., and Shaknovich, E. (1992) in *Protein Folding: Theoretical Studies of Thermodynamics and Dynamics in Protein Folding* (Creighton, T., Ed.) pp 126−195, W. H. Freeman, New York.
13. Bryngelson, J. D., Onuchic, J. N., Socci, N. D., and Wolynes, P. G. (1995) *Proteins: Struct., Funct., Genet. 21*, 167−195.
14. Dill, K. A., and Chan, H. S. (1997) *Nat. Struct. Biol. 4*, 10−19.
15. Chan, H. S., and Dill, K. A. (1988) *Proteins: Struct., Funct., and Genet. 30*, 2−33.
16. Bridgman, P. W. (1914) *J. Biol. Chem. 19*, 511−512.
17. Suzuki, K., Miyosawa, Y., and Suzuki, C. (1963) *Arch. Biochem. Biophys. 101*, 225−228.
18. Weber, G., and Drickamer, H. G. (1983) *Q. Rev. Biophys. 16*, 89−112.
19. Heremans, K., and Smeller, L. (1998) *Biochim. Biophys. Acta 1386*, 353−370.
20. Silva, J. L., and Weber, G. (1993) *Annu. Rev. Phys. Chem. 44*, 89−113.
21. Gross, M., and Jaenicke, R. (1994) *Eur. J. Biochem. 221*, 617−630.
22. Winter, R., and Jonas, J. (Eds.) (1999) *High-Pressure Molecular Science*, NATO ASI Series E, Vol. 358, Kluwer Academic Publishers, Dordrecht, The Netherlands.
23. Hummer, G., Garde, S., García, A. E., Paulaitis, M. E., and Pratt, L. R. (1998) *Proc. Natl. Acad. Sci. U.S.A. 95*, 1552−1555.
24. Winter, R., Erbes, J., Czeslik, C., and Gabke, A. (1998) *J. Phys.: Condens. Matter 10*, 11499−11518.
25. Panick, G., Malessa, R., Winter, R., Rapp, G., Frye, K. J., and Royer, C. (1998) *J. Mol. Biol. 275*, 389−402.
26. Panik, G., Vidugiris, G. J. A., Malessa, R., Rapp, G., Winter, R., and Royer, C. A. (1999) *Biochemistry 13*, 4157−4164.
27. Wlodawer, A., Borkakoti, N., Moss, D. S., and Howlin, B. (1986) *Acta Crystallogr. B 42*, 379−387.
28. Cook, K. H., Schmid, F. X., and Baldwin, R. L. (1979) *Proc. Natl. Acad. Sci. U.S.A. 76*, 6157−6161.
29. Schmidt, F. X., and Baldwin, R. L. (1979) *J. Mol. Biol. 135*, 199−215.
30. Schmid, F. X. (1983) *Biochemistry 22*, 4690−4696.
31. Udgaonkar, J. B., and Baldwin, R. L. (1988) *Nature 335*, 694−699.
32. Udgaonkar, J. B., and Baldwin, R. L. (1990) *Proc. Natl. Acad. Sci. U.S.A. 87*, 8197−8201.
33. Kiefhaber, T., Labhardt, A. M., and Baldwin, R. L. (1995) *Nature 375*, 513−515.
34. Howarth, O. W. (1979) *Biochim. Biophys. Acta 576*, 163−175.
35. Blum, A. D., Smallcombe, S. H., and Baldwin, R. L. (1978) *J. Mol. Biol. 118*, 305−316.
36. Holcomb, D. N., and Van Holde, K. E. (1962) *J. Phys. Chem. 66*, 1999−2006.
37. Benz, F. W., and Roberts, G. C. K. (1975) *J. Mol. Biol. 91*, 345−365; and 367−387.
38. Labhardt, A. M. (1982) *J. Mol. Biol. 114*, 181−293.
39. Labhardt, A. M. (1982) *J. Mol. Biol. 157*, 331−355.
40. Labhardt, A. M. (1982) *J. Mol. Biol. 157*, 357−371.
41. Seshadri, S., Oberg, K. A., and Fink, A. L. (1994) *Biochemistry 33*, 1351−1355.
42. Sosnick, T. R., and Trewhella, J. (1992) *Biochemistry 31*, 8329−8335.
43. Robertson, A. D., and Baldwin, R. L. (1991) *Biochemistry 30*, 9907−9914.
44. Desai, G., Panick, G., Zein, M., Winter, R., and Royer, C. A. (1999) *J. Mol. Biol. 288*, 461−475.
45. Takeda, N., Kato, M., and Taniguchi, Y. (1995) *Biochemistry 34*, 5980−5987.

46. Reis, O., Winter, R., and Zerda, T. W. (1996) *Biochim. Biophys. Acta 1279*, 5−16.
47. Siminovitch, D. J., Wong, P. T. T., and Mantsch, H. H. (1987) *Biochemistry 26*, 3277−3287.
48. Byler, D. M., and Susi, H. (1986) *Biopolymers 25*, 469−487.
49. Prestrelski, S. J., Byler, D. M., and Liebman, M. N. (1991) *Biochemistry 30*, 133−143.
50. Chen, M. C., and Lord, R. C. (1976) *Biochemistry 15*, 1889−1897.
51. Brandts, J. F., Oliveira, R. J., and Westort, C. (1970) *Biochemistry 9*, 1038−1047.
52. Yamaguchi, T., Yamada, H., and Akasaka, K. (1995) *J. Mol. Biol. 250*, 689−694.
53. Westmoreland, D. G., and Matthews, C. R. (1973) *Proc. Natl. Acad. Sci. U.S.A. 70*, 914−918.
54. Miller, W. G., and Goebel, C. V. (1968) *Biochemistry 7*, 3925−3935.
55. Fabian, H., and Mantsch, H. H. (1995) *Biochemistry 34*, 13651−13655.
56. Zhang, J., Peng, X., Jonas, A., and Jonas, J. (1995) *Biochemistry 34*, 8631−8641.
57. Wright, P. E., Dyson, H. J., and Lerner, R. A. (1988) *Biochemistry 27*, 7167−7175.
58. Moult, J., and Unger, R. (1991) *Biochemistry 30*, 3816−3824.
59. Kleppinger, R., Goossens, K., Loenzen, M., Geissler, E., and Heremans, K. (1997) in *High-Pressure Research in Bioscience and Biotechnology* (Heremans, K., Ed.), pp 135−139, Leuven University Press, Leuven, Belgium.
60. Phillips, C. M., Mizutani, Y., and Hochstrasser, R. M. (1995) *Proc. Natl. Acad. Sci. U.S.A. 92*, 7292−7296.
61. Backmann, J., Fabian, H., and Naumann, D. (1995) *FEBS Lett. 364*, 175−178.
62. White, A. J., Drabble, K., and Wharton, C. W. (1995) *Biochem. J. 306*, 843−849.
63. Reinstädler, D., Fabian, H., Backmann, J., and Naumann, D. (1996) *Biochemistry 35*, 15822−15830.
64. Olinger, J. M., Hill, D. M., Jakobsen, R. J., and Brody, R. S. (1986) *Biochim. Biophys. Acta 869*, 89−98.
65. Cléry, C., Renault, F., and Masson, P. (1995) *FEBS Lett. 370*, 212−214.
66. Peng, X., Jonas, J., Silva, J. (1990) *Proc. Natl. Acad. Sci. U.S.A. 90*, 1776−1780.
67. Nash, D. P., and Jonas, J. (1997) *Biochemistry 36*, 14375−14383.

BI992176N